GraF Integral Field and Long Slit Spectroscopy with the ESO 3.6m/ADONIS/SHARP system

A. Chalabaev[1], E. le Coarer[1], P. Rabou[1], Y. Mignart[1], P. Petmetsakis[1], D. Le Mignant[1,2]

[1] Laboratoire d'Astrophysique, Observatoire de Grenoble, BP 53X, F-38041 Grenoble Cedex, France

[2] European Southern Observatory, Casilla 16317, Santiago 19, Chile

Abstract - We present the test results of the GraF instrument built at Grenoble for spectro-imaging at high angular resolution with the ESO 3.6m/ADONIS and the 256x256 pixels SHARP camera. The instrument is operated in the 1.2 - 2.5 μm spectral range. It uses a Fabry-Perot interferometer (FPI) cross-dispersed with a grating, and provides the integral field spectroscopic capability, projecting on the detector several simultaneous monochromatic images of the field (windows). The necessity of such a capability for spectroscopy at high angular resolution is stressed and illustrated on test astronomical data and their deconvolution. The instrument provides 17 windows of 0.5" by 9" in the J band, 10 windows of 0.9" by 9" in the H band, and 8 windows of 1.5" by 12" in the K band, with the platescale of 0.035" in the J and H, and 0.05" in the K. The spectral resolution of windows is about 20000 in J, 10000 in H, and 7000 in K. The spectrum recorded in one exposure corresponds to the transmission pics of the FPI. The interorder space is covered in a sequence of exposures varying plate spacing of the FPI, providing a spectro-spatial cube of data equivalent to 1800^2 pixels. The instrument is easily modular. It converts to a classical long slit spectrograph, useful for observations of simple geometry objects such as binary stars, and to a direct imaging camera. This modularity proved to be very useful at the telescope, allowing to acquire in the same sequence the image, the long slit spectrum, and the $\{x, y, \lambda\}$ - map of the field. The measured limiting magnitudes in the spectro-imaging mode, for S/N = 5 and the exposure time 1 min, are respectively J/H/K = 8.5/9.4/9.3; in 5 min one gets J/H/K = 10.4/12.5/10.0. In the long slit mode, in 30 min exposure and with a high dispersion grating (300 mm^{-1}, R = 4000), one gets J/H/K = 12.1/12.9/11.5. With the low dispersion grating (35 mm^{-1}, R = 800) , available for the J and H bands, the limiting magnitudes are J/H = 14.5/15.4. The detector flat-field response, the instrumental thermal background, the point-spread function and the deconvolution results are presented and discussed. The instrument potential is illustrated by the data and astrophysical results obtained on a tight binary GU CMa and on the exploding star Eta Car.

1. Introduction

The design of the ESO ADONIS system (Beuzit et al. 1997) included the "visitor instrument bench", providing an important possibility of adding observational modes not foreseen or not initially budgeted. Spectroscopy with the adaptive optics was already offered by two SHARP camera pre-focal Fabry-Perot interferometers (FPI), with the spectral resolution R of 900 and 2300, operating in the K band by order selection and spectral scanning. However, a number of astronomical programmes required to extend these possibilities further to the J and H bands, and to a higher spectral resolution. For instance, a precise spectral classification of stars later than A is based on the metallic lines in the H band (cf. Dallier et al. 1996, Meyer 1996), while the typical velocity broadening for the lines of the circumstellar environment is often less than 100 km/s (see e.g. the spectro-imaging of planetary nebulae, Cox et al. 1997, or of the DG Tau jet, Lavalley et al. 1997), requiring R of 10,000 or more. The spectral specifications had to be combined with a reasonably large field of view not less than 1" - 2" at the shortest dimension, sampled at 0.035" and 0.05". These were the rather ambitious starting points of the GraF project (Chalabaev and le Coarer, 1994), which could be met only with an appropriate choice of the optical set-up for spectroscopy under adaptive optics.

Indeed, used in combination with high angular resolution technics, spectroscopy must necessarily have simultaneous imaging capability, already because the objects of interest are resolved, thus extended. Furthermore, the recorded image often exhibits features on a scale close to the angular resolution, so that "cleaning" for the instrumental point-spread function (PSF) of the experience is essential, implying the use of image restoration technics and the knowledge of the PSF. The latter, in the conditions of the ground based astronomy and in the spectral range under discussion, is known to suffer temporal variations at the time scale of minutes, or shorter, so that the use of image scanning technics in the focal plane, such as a long slit spectrograph, makes the subsequent image restoration unsure. The solution one naturally comes to is to record the flux distribution simultaneously on the $\{x, y, \lambda\}$ axes, using the technics of integral field spectroscopy, alias 3D-spectroscopy (hereafter 3Ds). In the frequently encountered case when the object is point-like in the continuum and extended only in selected wavebands (e.g. gas around a star or a galactic nucleus), the imaging over the wavelength spectrum provides the measurement of the angular PSF in the continuum simultaneously to the image of the extended emission recorded in the spectral line. This important advantage substantially reduces the level of the deconvolution artifacts (cf. the discussion of the difficulties of the time delayed PSF calibration elsewhere in these Proceedings).

However, the contiguous 3Ds technics, when the $\{x, y, \lambda\}$ data cube is recorded in one single exposure (Weitzel et al 1994, Bacon et al 1995, OASIS on Web; the Web references are given at the end of the article), are expensive in terms of the detector pixels number, and so far offer a modest FOV and/or spectral coverage. For instance, the VLT 3Ds instrument under adaptive optics SINFONI with a 1024^2 detector will have a FOV of 25 x 25 (SINFONI on Web), or 0.6" x 0.6" when sampled at half of the diffraction limit of the 8 m telescope. A contiguous 3Ds technic with the 256^2 pixels SHARP detector would give the field and/or spectral coverage far less than acceptable. Projecting a part of the $\{x, y, \lambda\}$ data cube on the time axis offers then a more appropriate solution. At this point, one can notice that contrary to the rapidly varying angular PSF, the spectral characteristics of the experience and of the object are in general slowly varying quantities, they can be calibrated on a hourly scale and recorded in a time sequence. The specifications of the FOV and of the number of spectral pixels we wished GraF meets led us to prefer a 3Ds set-up with partial projection of the spectral axis on a time sequence, namely a grating spectrograph cross-dispersed with a FPI. While the $\{x, y\}$ coverage of the field is contiguous in a number of "slot" windows (see Fig. 2), the λ-axis of one exposure is recorded only in several transmission pics of the FPI, the remaining spectrum being acquired in a series of exposures in 50 steps ("pixels") of the FPI. The overall spectro-spatial cube format $\{x, y, \lambda\}$ is therefore 256x256x50, or the equivalent of a 1800^2 detector. The typical values for the FOV are 30 x 256 pixels, with 8 spectral pixels acquired in one exposure, times 50 "pixels" projected on the time axis (see Section 2.1 for the wavelength dependance of the window parameters). The spectral resolution can exceed 10,000.

The instrument is compact, fitting into the small 1.5 m by 0.5 m room at the ADONIS visitor equipment bench, and into the light 30 kg weight budget. Further details can be found on the GraF Web page (referenced at the end of the article), in Chalabaev and le Coarer (1994, 1995) and le Coarer et al (1996). The set-up was originally described by Fabry (1905). Its integral field spectroscopic capability was noticed and first exploited by le Coarer et al. (1993).

In this paper, after a brief instrument description, we present the test results and first astronomy with GraF/ADONIS. It is one of the first integral field and long slit spectroscopy experience with the adaptive optics, and the lessons learned may be useful for future projects in the field.

2. Instrument Description

2.1 3D-spectroscopic capability

The GraF optical layout and the illustration of its 3Ds property are given respectively in Fig. 1 and 2. The FPI is placed in the parallel beam of the grating spectrograph after the focal rectangular aperture and the collimator, and in front of the grating. The FPI acts as a multi-passband quasi-monochromatic filter, removing the light in between its transmission pics and thus freeing the corresponding space for the image elements. The grating disperses the light passed by the FPI, and thus sorts the images of different colors on the detector. The images superimpose, with a wavelength shift corresponding to the FPI interorder, which, by means of the grating reciprocal dispersion and the imaging platescale, translates into the shift on the detector, and turns out to be the width of the free FOV. To avoid the confusion, the image width is therefore limited by the rectangular mask ("a large slit") in the spectrograph input focal plane. One can say that GraF is "a long and large" slit spectrograph. There is an absolute upper limit on the window width. Measured in the units of the angular resolution (one image element), this limit is equal to the FPI finesse, as one would expect since this is the number of spectral elements one payed off to get the imaging capability. For the finesse 20, and the image element 0.12" (3.6 m telescope, λ=2.2 μm), this gives the limit of 2.4". In practice, the dispersion is such that the FPI resolution element is dispersed on not more than 2 detector pixels, which gives, for the chosen FPI and grating parameters, the window width of 1.5" at λ=2.2 μm. The values of the FOV width for different wavelengths are summurized in Section 2.2. In the direction perpendicular to the spectral dispersion, the FOV is not affected, so that its height is given by the camera format and the platescale, being about 9" at 35 mas/pix and 12.8" at 50 mas/pix.

The spectral resolution is defined by the FPI plate spacing and the finesse. We use a Queensgate FPI with the plate spacing of 500 μm and with the finesse which varies around 20 in the spectral range from 1.2 to 4.6 μm, although the effective operation range of GraF is limited to 1.2 - 2.5 µm. The spectral resolution is about 7000 at 2.2 µm, about 12,000 at 1.7 µm and about 20,000 at 1.3 µm.

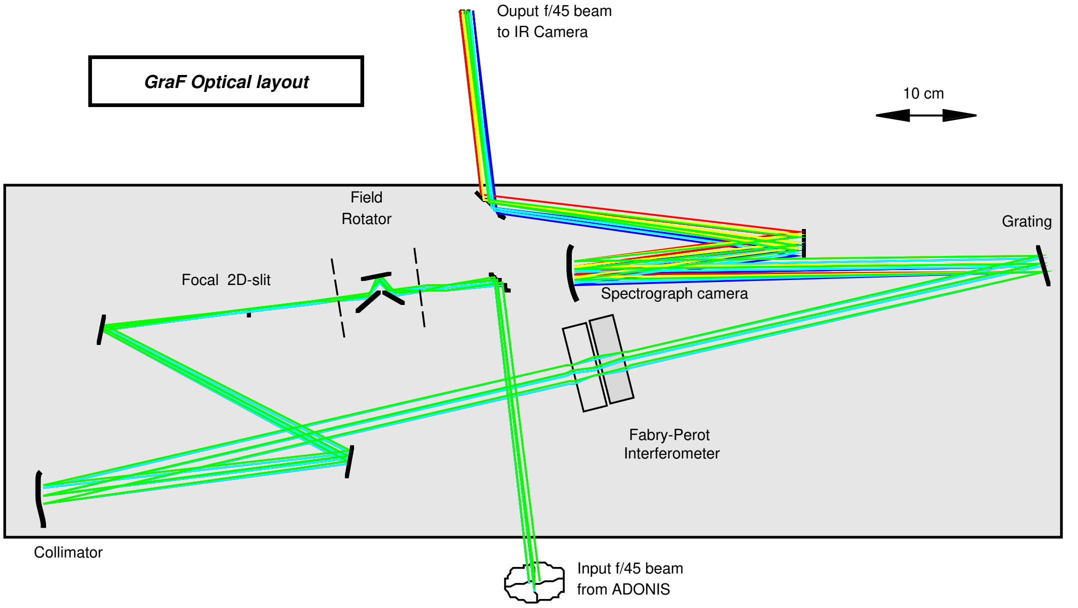

***Fig. 1** - The layout of the GraF implementation at the ADONIS visitor' bench. The dimensions of the spectrograph support (grey) are about 1.50 m by 0.50 m.*

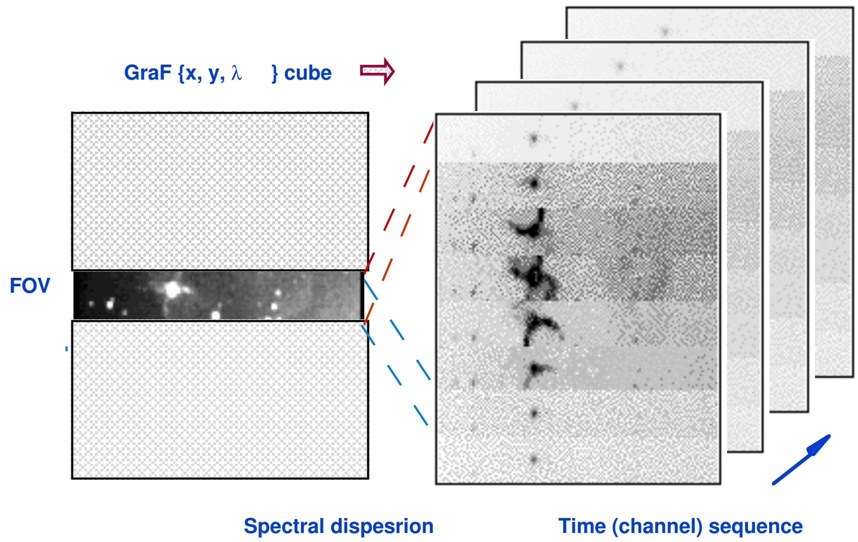

***Fig. 2** - The illustration of the integral field spectroscopic capabilty of the grating + Fabry-Perot interferometer set-up. The image of the field in several monochromatic passbands, corresponding to the FPI transmission pics, is recorded in one exposure. The entire {x, y, λ} - cube is formed by a series of exposures at different FPI spectral settings.*

Finally, let us to mention two advantages of the FPI cross-dispersed with a grating with the respect to the classical scanning FPI with order selection. The first one is the monitoring of the channel-to-channel photometric variations on the continuum spectrum of the object. Imposing invariance of the continuum emission allows to correct for the variations as illustrated in Fig. 3. The second one is more subtle, it is related to the contamination of the selected order by the emission in the adjacent orders. The effect is particularly troublesome if one measures a faint absorption feature in the selected order with a strong emission present in the adjacent orders. Sorting the orders by cross-dispersion allows a more clear monitoring of the possible contamination.

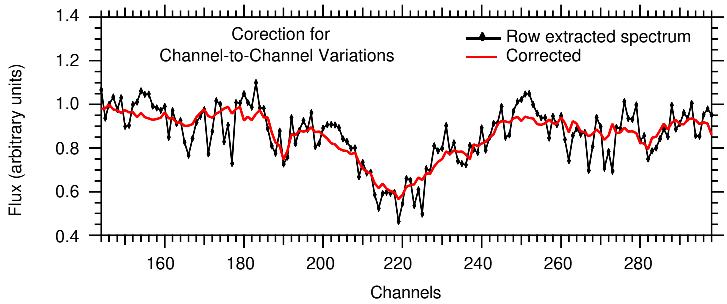

Fig. 3 *- A spectrum of the Brγ line in a standard starr, extracted from a 3Ds GraF scan. Channel-to-channel signal variations (solid-dotted line) are corrected imposing invariance in average of the signal in the continuum (solid line). The star is HR8353, B8III, K = 3.3, exposure time per channel 10 s, taken on Nov 14, 1997.*

2.2 Observing modes

Removing the FPI out of the beam converts the instrument in a classical long slit (LS) grating spectrograph. Although the spatial information along one of the axes is lost, this free of scanning fast mode is useful for objects of simple geometry, mainly binary stars. It is also helpful as a cross-calibration spectrum for the 3Ds cube.

Finally, turning the grating in the zero-order position, or replacing it by a flat mirror, converts the instrument in the imaging mode, used during alignments, target acquisition, fine pointing, and imaging.

The parameters of the 2 spectroscopic modes are summarized in the table below. The limiting magnitudes are given in Section 3.6, and the observing procedure is presented in Section 4.

3Ds mode	**Long Slit mode**
R = 7000-25000 (decreasing with λ) FOV : J : 0.6” x 9” H : 0.8” x 9” K : 1.5” x 12” Exposure time per channel: 1 - 5 min Number of channels : 10 - 50 Cube acquisition time: 20 - 60 min	Gratings : 300 et 600 mm^{-1} Parameters @λ = 2.2 µm - 300 mm^{-1}, disp = 0.15 nm/px, R = 3700 - 600 mm^{-1}, disp = 0.06 nm/px, R = 7000 Typical exposure time: 1 - 30 min

2.3 Implementation at ADONIS

The GraF instrument is mounted at the "visitor bench" of ADONIS, fitting in the space about 150x50 cm (Fig. 1). A flat mirror deviates the ADONIS f/45 beam into GraF, and another flat mirror sends the GraF processed beam within nominal specifications to the SHARP camera. The two mirrors are mounted on the same support with precise positioning. Removing the mirrors is a simple operation, allowing if necessary regular ADONIS imaging observations.

The instrument control electronics box is mastered by the ADOCAM software, written by F. Lacombe. The GraF version of ADOCAM includes the usual ADONIS observer commands (On-Off mirror movements, SHARP camera optics, detector exposure, display, etc.) and the commands specific to GraF (slit width, FPI in and out, FPI scanning, grating movements).

3. Test results

3.1 General

After the lab tests at Grenoble, GraF was extensively studied with ADONIS/SHARP in the lab at La Silla, and finally tested on the sky with 3.6 m telescope/ADONIS/SHARP during 4 nights in July and November 1997. The conclusions worthwhile to mention here are the absence of optical quality degradation within the nominal 12.5"x12.5" field, the mechanical flexures low enough to allow exposures up to 1 - 2 hours, and the low level (0.5%) and clear separation of the ghosts in the 3Ds mode. The wavelength calibration and the spectral settings showed to be stable.

The detector properties, namely the dark charge on long exposures, the response calibration on the flat-field, and the instrumental thermal background are discussed in more details below. Let us to mention here that the "cosmetic" properties of the NICMOS chip, in particular the sporadically "hot" and "dead" pixels make the data reduction sometimes cumbersome, and always time consuming.

3.2 Detector Dark Charge and Response on a Flat Field

The dark frames of the SHARP detector with the exposure time longer than about 5 min, taken in a series, exhibit different levels (see Fig. 4). The possible reasons are the imperfect charge transfer, or/and cooling of the detector with no light on from one dark exposure to the next one. Consequently, the procedure established to obtain the darks useful for the data reduction consists in exposing the detector to the instrumental emission before obtaining a dark frame, which is close to the conditions of the exposures on the sky.

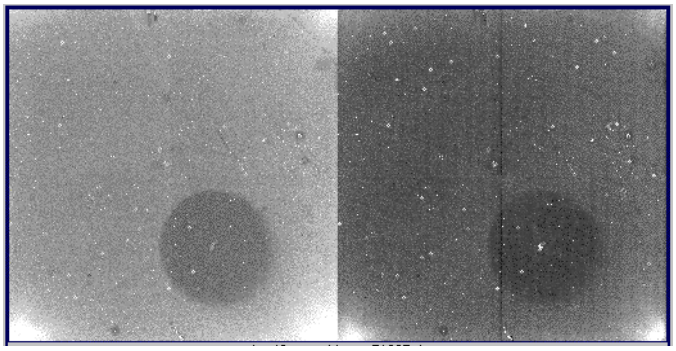

Fig. 4 *- Two subsequent dark exposures of the SHARP detector with t = 5 min. The median value is 26 ADU above the bias for the first exposure, and 4 ADU for the second one. The dark circle, known as "the SHARP eye", is a faint feature probably due to a lower charge transfer efficiency in this region.*

Flat-field (FF) calibration exposures are obtained by illuminating the ADONIS entrance pupil with a white lamp. The resulting images are shown in the Fig. 5. Besides the usual pixel-to-pixel sensitivity variations, the FF's display a well visible system of fringes, with the period about 50 pix, formed most plausibly by the interference of the light reflected at the sapphire plate of the NICMOS detector. There is also a second system of fringes with the period of about 4 pixels, formed probably by the interference of light reflected on the surfaces of the cryostat window.

The different appearance of the fringe system in the LS and the 3Ds modes is due to the different evolution of the wavelength along the detector. In the LS mode, the wavelength of the incident light varies continuously along the columns, while in the 3Ds mode this variation is a step function. The amplitude of the fringe modulation may be as high as 15% pic-to-pic, and the proper FF calibration is of course important. At the telescope, a FF is obtained for each object both in the 3Ds and LS modes.

It was found that the simple object by flat-field frame division give satisfaction in the 3Ds mode, resulting in undetectable residual fringing. This was not always the case for the LS spectra. The analysis of the observing and FF calibration procedures showed that the reason of the FF-ing failure was the insufficient centering of the stellar object on the slit. Here, we must describe in more details the observing and calibration procedure. The way we avoid to deal with possibly non-trivial image transfer function of a slit, and also to decrease the light loss, is to open the slit wide (typically 0.4") and let the stellar image profile across the dispersion (typically 0.2" at FWHM) to play the role of the slit. Subsequent FF calibrations are done for a series of slit width (0.2", 0.3", 0.4") to isolate the "sapphire" (period of about 50 pix) and "cryostat window" fringes (period about 4 pixels). Obviously, if the stellar object is not centered perfectly within the slit, its system of fringes has a phase lag with the respect to the FF fringes. Then the FF calibration frame is processed in the following way before the division. By an adapted filtering, we separate the variations due to the fringes (period of about 50 pix) from the pixel-to-pixel variations (high frequencies), as well from the slow variations due to the filter transmission. After changing the phase of the extracted fringe function, it is recombined back with the high and low frequencies contributions. Of course, a proper centering on the slit, which is possible with ADONIS down to 10-20 milli-arcsec precision, makes the data reduction more straightforward. However, objects of a complicated geometry with uneven distribution of energy across the slit will necessarily have varying fringe phase. This fact must be taken into account before the observer decides to use the apparently simple long slit spectroscopy under adaptive optics.

The high frequency "cryostat window" fringes are badly eliminated by the simple object to flat-field division. A special data reduction procedure of extraction of the fringe system remains to be developed. Given that the amplitude of these fringes is low and the frequency is high, so far a simple smoothing is applied to remove them, albeit at the price of a small spectral resolution loss.

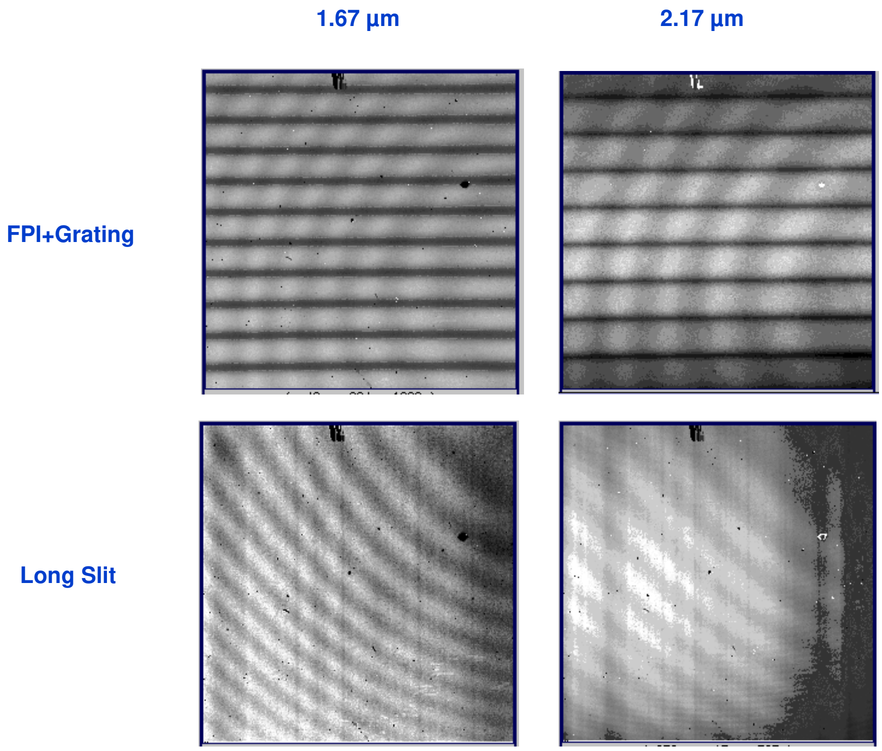

Fig. 5 *- Flat field exposures in the 3Ds mode (above) and in the long slit mode (below), taken at 1.67 µm with the large band H filter and at 2.2 µm with the narrow-band CVF filter.*

Let us come back to the formation mechanism of the "sapphire" fringes. As we suggest, the pattern is formed by the interference of light reflected on the sapphire substrate of the NICMOS detector. The 50 pix period fringe modulation over the detector surface is then due to the fact that the beams from the SHARP objective, corresponding to different points of the focal plane, have slowly varying incidence angle, and therefore the path difference. A simple simulation of this interference scheme reproduces the fringes as shown in Fig. 6 for the long slit mode. Choosing a camera design eliminating the fringing effect in monochromatic light is certainly possible, and we strongly recommend this point to be included into specifications of camera designs.

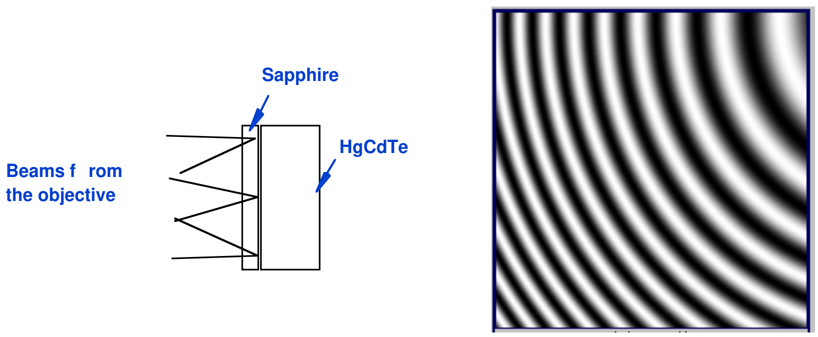

Fig. 6 *-* ***Left****: Schematic of the fringe formation by the objective and sapphire substrate.* ***Right*** *: Simulated fringes in the long slit mode.*

3.3 Point-spread function and the "adaptive optics bumps"

In the 3Ds mode, for a given GraF window, the output ADONIS "white" PSF is multiplied in the spectral domain by the FPI transmission and dispersed by the grating. The final PSF is elongated in one direction. The grating dispersion is chosen so that the FWHM of the FPI transmission pic corresponds to about 2 pixels on the detector, the actual value depending on the used spectral range. This additional convolution reduces the angular resolution along the axis of dispersion, however the effect seems to be weak, especially if the image can be deconvolved by the PSF in the continuum windows.

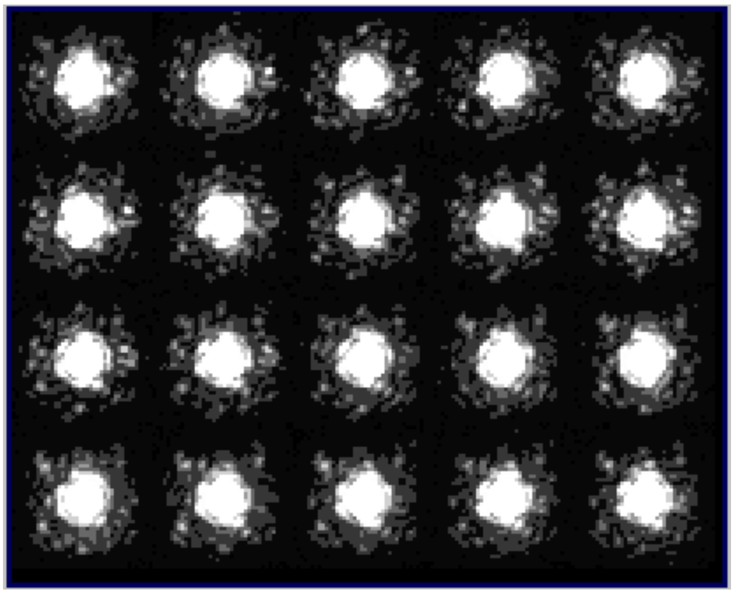

Fig. 7 *- A sequence of 20 direct images with the exposure time of 1 s, taken on Nov 15, 1997, and illustrating the ADONIS "bumps", or "the adaptive optics speckles", and their temporal evolution. The halo of "bumps" is at 1-3% of the maximum. The time sequence is from left to right, and from up to down.*

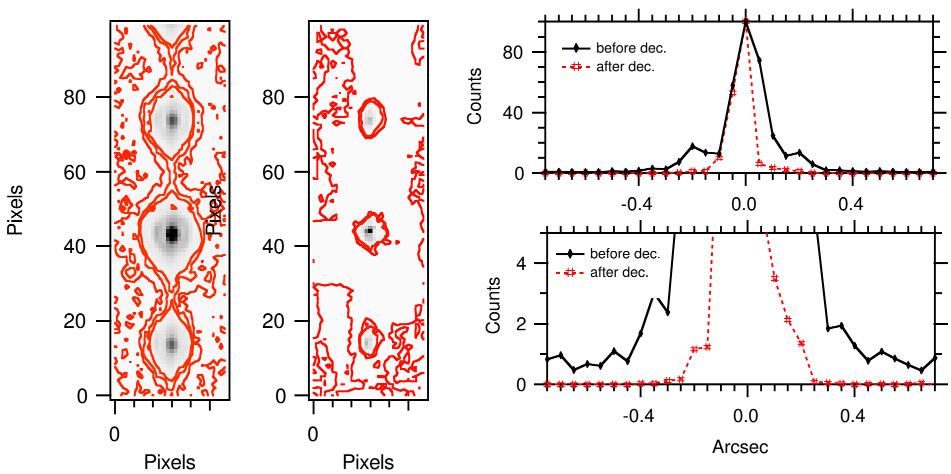

Fig. 8 *- Elimination of the instrumental halo (diffraction rings and "bumps") by deconvolution. The object is HR Car, exposure 120 s, 1 frame out of 20 frames scanned around 2.1655 µm, Nov 16, 1997. The images are normalized to the maximum. The central window is on the Brγ line the two adjacent windows are on the continuum.* ***Left****: before deconvolution, contours are at 0.5, 1 and 1.5% above the background level.* ***Right****: after deconvolution (see text), similar countour levels.* ***Plots****: Signal the maximum, plotted in two flux scales.*

The example given in this section shows that indeed such a deconvolution eliminates quite properly not only the elongation, but also the diffraction rings and, quite importantly, the "adaptive optics bumps" (or the "adaptive optics speckles", see elsewhere in these proceedings). The latter are troublesome in astronomical studies of faint knots and haze, as illustrated in a sequence of the ADONIS output PSF given in Fig. 7. A halo of the "bumps" at 1-3% of the maximum and their temporal evolution are well seen. The Fig.8 shows the GraF window images before and after deconvolution. The object, HR Car, has a strong emission in the hydrogen 2.1655 µm Brγ line, the flux at the maximum being about twice that of the continuum. The central window is centered on the hydrogen emission, the two other windows being at the adjacent continuum. These windows display the elongated PSF (Fig.8, left image) . The contours at the very low level (0.5, 1 and 1.5 % above the background) show the halo due to the seeing and the "bumps". After the deconvolution, using the PSF of the continuum, and 10 iterations of Lucy algorithme (Lucy 1974), the halo around the stellar image is reduced to the level less than 1% of the maximum outside the cercle of 0.2" of radius, and less than 0.1% outside the cercle of 0.25" (cf. Fig. 8, right image, and plots).

Another example of a successful deconvolution of the GraF data, obtained on an astronomical object of a complex but well known geometry (Eta Car) is discussed in Section 5.

3.4 Thermal background in the K-band

With the low level of the read-out noise (RON) of modern detectors, observations in the K-band may be limited by the photon noise of the instrumental thermal background. This is particularly true for a grating spectrograph at ambient temperature. The limited mechanical room and weight budget on the ADONIS visitor bench excluded implementation of cooling. On the other hand, given the high spectral resolution used and the small spectral range covered at one setting, the background radiation on the detector can be reduced using a cooled narrow-band filter for observations in the K-band. The estimates showed the penalty in the limiting magnitudes being still acceptable (le Coarer et al 1996). Finally, the instrumental background flux, measured on a blank sky at λ=2.2 µm, was found even less than the project conservative estimates, and equal to 100-120 ADU in 1 min (or about 1000 photons/min), both in the LS and 3Ds modes with the CVF as the blocking filter. The corresponding noise is 3.4 ADU (cf RON = 3.7 ADU, or 35 e). Thus, for exposures less than 1 min, the GraF observations are RON limited. Note that 1 min is the recommended exposure time for the 3Ds mode. For exposures longer than 3 minutes, relevant for observations in the LS mode, the noise is dominated by the thermal background. The limiting magnitude is penalized by 1.3 mag for the typical deep LS exposure time of 30 min.

3.5 Limiting magnitudes

The measured at telescope limiting magnitudes are given in the Table below for two S/N ratios corresponding to detection of faint features and to quantitative spectroscopy, for conservative AO correction values (SR=0.2-0.3). The figures are given for the 300 mm^{-1} grating. For the 35 mm^{-1} grating (long slit mode only), add 2-2.5 mag, and for the 600 mm^{-1} grating, subtract 0.75 mag in J and H, and 0.4 mag in K.

The instrument efficiency is very close to the theoretical estimate (le Coarer et al. 1996), i.e. 50% in the worst case of the 3Ds mode, when all optical parts are in the beam. In the J and H bands, the dominating noise at low flux levels is that of the read-out. In the K band, as we already mentioned, this is also the case for exposures less than 1 min, and for exposures longer than 3 min, the dominating noise is due to the thermal background.

Mode	Exp.time min.	J		H		K	
		S/N=5	S/N=30	S/N=5	S/N=30	S/N=5	S/N=30
3Ds	1	8.5	6.7	9.4	7.5	9.3	7.3
	5	10.4	8.5	12.5	10.0	10.0	8.0
Long Slit	5	10.6	8.7	11.4	9.5	10.6	8.5
	30	12.1	10.2	12.9	11.0	11.5	9.6

4. Observing procedure and time budget

In the 3Ds mode, a typical set of observations consists of the following exposures:

- direct image of the field
- long slit flat-field
- long slit wavelength calibration
- long slit spectrum of the object
- 3Ds flat-field cube
- 3Ds wavelength calibration cube
- 3Ds cube of the object

The indicative time budget and the observing sequence are as follows:

1. LS only dataset, typical total time (and possible range)	20 min (15-40 min)
Overhead total:	ca. 10 min
- Telescope pointing, grating setting, Calibration lamps On	3 min
- LS Flat-field frame, WCal frame	3 min
- ADONIS loop closure	3 min
Typical Object exposure time:	5-30 min
2. 3Ds dataset, typical total time (and possible range):	60 min (40 - 90 min)
Overhead total:	15-20 min
- Telescope pointing, grating setting, Calibration lamps On	3 min
- LS Flat-field frame, WCal frame	3 min
- 3Ds cube Flat-field cube, WCal cube	6 min
- ADONIS loop closure	3 min
- FPI channel-to-channel overhead	ca. 10 s
Typical Object exposure time per channel:	0.5-3 min
Typical number of channels:	15-50
Typical data cube acquisition time:	20-70 min
Special overhead : FPI plates parallelism adjustment (end of afternoon and middle of night)	10 min

5. First Astronomy with GraF/ADONIS

During the last test nights we observed a sample of objects prototypical of the GraF/ADONIS programmes. Two of them are presented here.

A tight binary GU CMa, supposed to belong to the class of the Ae/Be Herbig stars, was previously studied with ADONIS JHK imaging by Corporon (1998). He measured the separation of 0.66", and the K magnitudes of 6.58 and 8.08 respectively for the primary and secondary components. The GraF long slit frame at $\lambda = 2.1655$ µm and the extracted spectra are shown in the Fig. 9. The primary exhibits the hydrogen Brγ line in emission, while the secondary has a photospheric absorption line. It appears surprising that the binary components, supposingly formed together and having similar masses (sp. class B deduced from to the spectral distribution of energy, Corporon 1998), have such a significant difference in brightness and spectrum. A plausible explanation, as suggested by Yudin (1998), is that the primary is a classical Be stars, implying an evolved status for GU CMa rather than the pre-main sequence status of Ae/Be Herbig stars.

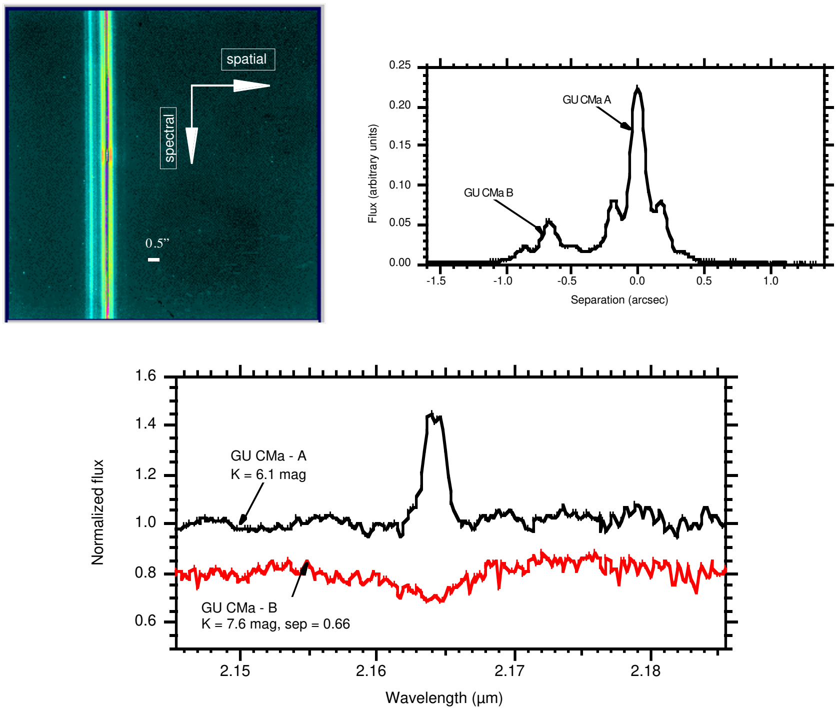

***Fig. 9 - Upper left** : ADONIS/GraF long slit spectrum of a binary star GU CMa (K1=6.1, K2 = 7.6, separation 0.66"). The exposure time 5 min, grating 300 gr/mm, spectral resolution of about 5000, setting 2.1655 μm, S/N = 60. **Upper right :** The plot of the signal in the spatial direction. Note the presence of dispersed diffraction rings and clear separation of the components. **Bottom:** Reconstructed spectra of the companions. Note that only the primary shows the hydrogen Brγ emission. The residual fringing on the primary spectrum is reduced by flat-fielding from the initial 10% (typical of NICMOS array used in monochromatic light) down to less than 1% amplitude. The spectrum of the secondary is shifted down by 0.2.*

The second example is the 3Ds data of Eta Car, the exploding star, believed to represent the LBV, or similar phase in the evolution of (very) massive stars (cf. review by Davidson and Humphreys 1997). Besides the immediate astronomical interest, this object is one of the best targets to test the high angular resolution instrumentation. This is due to the presence of secondary spots to the NW from the central star at the distance of only 0.1"-0.2" (Hofmann and Weigelt 1988), and to the SE at the distance of 0.5" (Rigaut and Gehring 1995). Helpfully, a spatially resolved spectroscopy of the secondary spots done with the HST is also available (Davidson et al. 1995). The challenge for GraF/ADONIS was further reinforced by the choice of the H band, where the adaptive optics correction becomes only partial with the Strehl ratio not more than 0.5. We discuss these data in more details in a separate paper of these proceedings (Chalabaev, Le Mignant, and le Coarer), and give here only brief summary. We choose the spectral range around of 1.68 μm, with the lines of hydrogen Br11, [FeII] 1.6769 μm, and FeII lines at 1.6783 μm and at 1.6873 μm (Hamann et al. 1994). In all these lines, the long slit spectrum exhibits a spatially extended emission with different evolution to the NW and SE. So far, only 1 frame out of the 48 frames of the 3D cube was deconvolved, to study the deconvolution in the conditions close to the GraF/ADONIS limits. The frame corresponds to the maximum of emission in the FeII 1.6783 μm line, where the contrast of the secondary spots with the respect to the central star is the best (see Fig. 10). The spectral passband of windows is 0.17 nm (R = 10,000). The continuum sub-image at 1.6704 μm was used as the PSF for the maximum likelihood iterative deconvolution (Lucy 1974). A simple regularisation was done by stopping the process at 200 iterations. No artifacts appear at least at the level of 0.05% of the maximum, while the achieved resolution FWHM = 0.1" is close to the diffraction limit. In the continuum 1.6760 μm window, the image appears as a point-like circular source. In the 1.6676 μm and 1.6731 μm windows, it shows some extension at levels less than 0.05% of the maximum. It must be investigated further whether we deal with real extended features emitting in faint lines, or with the deconvolution artifacts at a low level. The secondary NW spots, although glued together at this angular resolution, are clearly present to the right of the central star in the windows corresponding to the strong FeII emission lines, and noticeably absent in the Br11 window, confirming the implications derived from the long slit data, and suggesting a different nature of the emission to the NW and to the SE, with more reflexion/scattering and a higher dust/gas ratio to the SE.

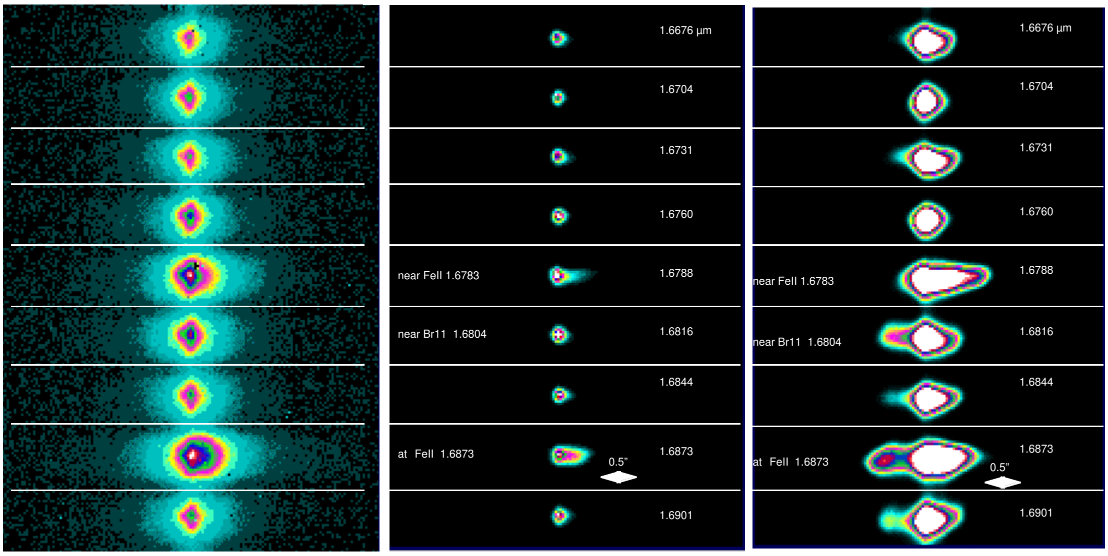

Fig. 10 - A 3Ds frame of Eta Car illustrating the deconvolution results with the PSF measured in one of the continuum windows. The exposure time 5 s, the frame, corresponding to the maximum of emission in FeII 1.6873 µm line was extracted from the cube of 48 frames taken on Nov 14,1997. The windows are 0.9" x 9" with the spectral passband of 0.17 nm. ***Left*** *: before deconvolution.* ***Right*** *: after deconvolution, linear scale of flux.* ***Middle*** *: same, log scale enhancing the very low flux levels.*

6. Conclusions

The first experience of using the grating spectrograph cross-dispersed with a Fabry-Perot interferometer in the conditions of the adaptive optics gives satisfaction. The set-up allows to obtain the spectroscopy at resolution of about 10,000 over the field of about 2"x12" sampled at 50 mas, with the angular PSF recorded simultaneously in the continuum windows. The subsequent deconvolution of a test object shows the proper recovery of the image angular flux distribution down to 0.1" scale in the H band, i.e. close to the telescope diffraction limit, even in the conditions of a low Strehl ratio.

The long slit spectroscopy, well adapted for observations of binaries, needs a careful observing procedure to keep the instrumental interference fringes from the object in phase with those from the calibration source. By this reason, the long slit spectroscopy, albeit appearing simple, may become cumbersome if applied to the objects of complex geometry with an uneven flux distribution across the slit.

A regular GraF observations started in May 1998, with 23 nights allocated by the ESO Observing programme Committee to 8 programmes in the one year period (April 1998 - Mar 1999), illustrating the strong scientific case of the observations combining high angular resolution with spectroscopy.

Acknowledgments

It is a pleasure to thank many people at Laboratoire d'Astrophysique de l'Observatoire de Grenoble (LAOG) and elsewhere for discussions and help. F. Lacombe wrote additional code of the ADOCAM control software making possible GraF and SHARP interaction; E. Stadler helped with the mechanics; C. Tran-Tiet, and G. Duvert contributed to the data reduction software, R. Conan and E. Zubia to the numercial simulations, H. Lanteri and C. Aime advised on the data deconvolution, C. Perrier, N. Hubin, J.-L. Beuzit, R. Gredel, S. Gilloteau, R. Petrov, P. Léna, J. Melnick, G. Monnet have been advising all along the project advancement; J. Bouvier, T. Böhm, J. Eislöffel, C. Dougados contributed to the scientific case of the GraF proposal document, the ESO La Silla staff, in particular J. Roucher, E. Barrios, J. Fluxa, A. Gilliotte, F. Marchis, M. Maugis, V. Merino, P. Prado, A. Sanchez, R. Tighe, was extremely helpful during the GraF tests at the 3.6m telescope. The funding was provided by CNRS/INSU/MENSR/Programme National de Haute Résolution Angulaire en Astronomie, Région Rhône-Alpes, LAOG and Observatoire de Grenoble. Scientific collaborations budget is partially supported by the grants from GdR "Milieux circumstellaires". The telescope technical time was provided by ESO. DLM is thankfull to "Société des Amis des Sciences" for the studentship which made possible his stay at Grenoble.

References

Bacon, R., Adam, G., Baranne, A., Courtes, G., Dubet, D., Dubois, J.P., Emsellem, E., Ferruit, P., Georgelin, Y, Monnet, G., Pecontal, E., Rousset, A., Say, F, 1995, "3D spectrography at high spatial resolution. I. Concept and realization of the integral field spectrograph TIGRE", A&AS, 113, 347

Beuzit, J.-L., Demailly, L., Gendron, E., Gigan, P., Lacombe, F., Rouan, D., Hubin, N., Bonaccini, D., Prieto, E., Chazallet, F., Rabaud, D., Madec, P.-Y., Rousset, G., Hofmann, R., Eisenhauer, F., 1997, "Adaptive Optics on a 3.6-Meter Telescope. The ADONIS System.", ExA, 7, 285

Chalabaev A., and le Coarer, E., 1994 : “GraF for ADONIS: Proposal of 3D spectro-imaging option for the ESO adaptive optics system", LAOG, Rapport téchnique n° 1

Chalabaev, A., and le Coarer, E., 1995 : "Astronomical potential of the Fabry-Perot Interferometers used in the multi-channel mode", in Proc. of ESO Workshop “Science with the VLT”, ed. J. Walsh et I.J. Danziger, Garching, 28 June - 1 July 1994, Suppl. Vol. p. 135

le Coarer, E., Chalabaev, A., Rabou, P., Magnard, Y., Petmetzakis, P., 1996, "GraF Instrument description", LAOG Rapport Technique n° 6

Corporon, P., 1998, PhD Thesis, Université Joseph-Fourrier, Grenoble

Cox, P., Maillard, J.-P., Huggins, P.J., Forveille, T., Simons, D., Guilloteau, S., Rigaut, F., Bachiller, R., Omont, A., 1997, "Molecular hydrogen morphology, kinematics and excitation in AFGL 2688 and NGC 7027", A&A, 321, 907

Dallier, R., Boisson, C., and Joly, M., "A library of H band stellar spectra for tsellar population analysis purposes", A&AS, 116, 239

Fabry, Ch., 1905 : C.R. Acad. Sci. Paris, 140, p.848

Davidson, K., Ebbets, D., Weigelt, G., Humphreys, R. M., Hajian, A. R., Walborn, N. R., Rosa, M. 1995, "HST/FOS spectroscopy of Eta Carinae: the star itself, and ejecta within 0.3 arcsec", AJ, 109, 1784

Davidson, K., and Humphreys, R. M. 1997, "Eta Carinae and Its Environment", ARAA, 35, 1

Hamann, F., Depoy, D. L., Johansson, S., and Elias, J. 1994, "High-resolution 6450-24500 A spectra of Eta Carinae", ApJ, 422, 626

Hofmann, K.-H., and Weigelt, G. 1988, "Speckle masking observation of Eta Carinae", A&A, 203, L21

Lavalley, C.; Cabrit, S.; Dougados, C.; Ferruit, P.; Bacon, R., 1007, "Sub-arcsecond morphology and kinematics of the DG Tauri jet in the [O I] 6300 A line", A&A, 327, 671

Lucy, L. B. 1974, AJ, 79, 745

Meyer, M. R. 1996, "The Stellar Populations of Deeply Embedded Young Clusters: Near-Infrared Spectroscopy and Emergent Mass Distributions", PASP, 108, 38

le Coarer, E., Georgelin, Y.P., and Boulesteix, J., 1993, CFHT Bull. 29, p. 14

Rigaut, F., and Gehring, G. 1995, "The inner core of Eta Carinae in the near-infrared", Rev. Mex. A. A., Conference Series, 2, 27

Weitzel, L., Cameron, M., Drapatz, S., Genzel, R., Krabbe, A., 1994, "3D: The New MPE Near-Infrared Field Imaging Spectrometer", ExA, 3, 317

Yudin, R., 1998, personal communication

Web References

GraF spectro-imager, http://www-laog.obs.ujf-grenoble.fr/hra/graf/

OASIS integral field spectrograph, http://www-obs.univ-lyon1.fr/~oasis/home/index.html

SINFONI integral field spectrograph, http://www.eso.org/instruments/sinfoni/